Supplementary Figure legends

Figure 1. RNA-Seq transcriptome analysis of fxSCA7 92Q mice, and validation of calcium homoestasis gene expression alterations at the protein level in fxSCA7 92Q mice. [Related to Figure 1]

(A) We isolated RNAs from the cerebellum of presymptomatic (12 week-old) and symptomatic (29 week-old) fxSCA7 92Q mice (SCA7; n = 3 / time point) and non-transgenic littermate controls (WT; n = 3 / time point), and performed RNA-Seq analysis, which yielded 100 differentially expressed genes (DEGs). Hierarchical clustering of the 100 DEGs is shown.
(B) ITPR3 immunoblot analysis of cerebellar lysates from 42 week-old fxSCA7 92Q and WT mice (n = 3 / group). GAPDH immunoblot served as a loading control. Bottom: quantification of ITPR3 protein expression normalized to GAPDH. Two-tailed *t*-test, $^{**}P < 0.01$
(C) IP3KA immunoblot analysis of cerebellar lysates from 42 week-old fxSCA7 92Q and WT mice (n = 3 / group). GAPDH immunoblot served as a loading control. Bottom: quantification of IP3KA3 protein expression normalized to GAPDH. Two-tailed *t*-test, $^{*}P < 0.05$
(D) $Ca_v3.1$ immunoblot analysis of cerebellar lysates from 40 week-old fxSCA7 92Q and WT mice (n = 3 / group). Tubulin immunoblot served as a loading control. Bottom: quantification of $Ca_v3.1$ protein expression normalized to tubulin. Two-tailed *t*-test, $^{**}P < 0.01$
Error bars = s.e.m.

Figure 2. Characterization of aberrant Purkinje cell electrophysiology in SCA7 mice. [Related to Figure 2]

(A) We performed immunostaining for $Ca_v3.1$ in the posterior cerebellar lobules of 25 week-old fxSCA7 92Q and WT mice (n = 6 - 8 / group), and observed a significant reduction in $Ca_v3.1$ fluorescence intensity in fxSCA7 92Q mice. Two-tailed *t*-test, $^{***}P < 0.001$
(B) We performed immunostaining for calbindin in the posterior cerebellar lobules of 25 week-old fxSCA7 92Q and WT mice (n = 3 / group), and observed a significant reduction in calbindin fluorescence intensity in fxSCA7 92Q mice. Two-tailed *t*-test, $^{*}P < 0.05$
(C) To quantify Purkinje cell neuron loss, we measured linear Purkinje cell density in the anterior and posterior cerebellum of 25 week-old fxSCA7 92Q and WT mice (n = 5 / group).

Purkinje cell number was unchanged in the anterior and posterior cerebellum of SCA7 mice at this time point. Two-tailed t-test, *P* = n.s. (not significant)

(D) Acute cerebellar slice recordings from the posterior cerebellum of 25 week-old fxSCA7 92Q and WT mice shown in **Figure 2E** are plotted here as a binned frequency histogram to better show the right shift of the distribution of ISI CV of Purkinje cell firing in fxSCA7 92Q mice.

(E) Purkinje cell firing frequency is unchanged between fxSCA7 92Q and WT mice (n = 5-6 / group) in both the anterior and posterior cerebellum of WT and fxSCA7 92Q at 14 weeks of age. WT cells: n = 22-38, fxSCA7 92Q cells: n = 19-25. Two-tailed t-test, *P* = n.s.

(F) Purkinje cell firing frequency is unchanged between fxSCA7 92Q and WT mice (n = 4-5 / group) in both the anterior and posterior cerebellum of WT and fxSCA7 92Q at 25 weeks of age. WT cells: n = 29-32, fxSCA7 92Q cells: n = 19-24. Two-tailed t-test, *P* = n.s.

(G) Purkinje cell firing frequency is unchanged between fxSCA7 92Q and WT mice (n = 5-7 / group) in both the anterior and posterior cerebellum of WT and fxSCA7 92Q at 40 weeks of age. WT cells: n = 29-34, fxSCA7 92Q cells: n = 41-49. Two-tailed t-test, *P* = n.s.

(H) Data corresponding to **Figure 2H**, which indicate no change in input resistance between fxSCA7 92Q and WT Purkinje cells. WT cells: n=9, fxSCA7 92Q cells: n=11; two-tailed t-test, *P* = n.s. Error bars = s.e.m.

Figure 3. Combined action of BK and T-type calcium channels regulate Purkinje cell spiking, and Fluo-4 treatment of primary cerebellar granule neurons. [Related to Figure 2]

(A) T-type calcium channel Ca_v3 subfamily blockade alone (4 μM mibefradil) does not cause spiking irregularity in WT Purkinje cells from the posterior nodular zone of the cerebellum. n = 6 cells; two-tailed *t*-test, *P* = n.s.

(B) BK channel blockade alone (100 nM iberiotoxin) does not cause spiking irregularity in WT Purkinje cells from the posterior nodular zone of the cerebellum. n = 8 cells; two-tailed *t*-test, *P* = n.s.

(C) Simultaneous blockade of BK channels and T-type calcium channel Ca_v3 subfamily (iberiotoxin 100 nM + mibefradil 4 μM combined) produces irregular Purkinje cell spiking in the posterior nodular zone of the cerebellum of WT mice. n = 11 cells; two-tailed *t*-test, $^{**}P < 0.01$.

(D) Representative acute cerebellar slice recordings from the posterior nodular zone of WT mice, showing Purkinje cell spiking before (left) and after (right) perfusion of 4 μM mibefradil (Mibef) and 100 nM iberiotoxin (Ibtx). Irregular spiking is indicated with red carats.
(E) Validation of Purkinje cell neuron transduction. Representative confocal fluorescent images of posterior nodular zone of the cerebellum in a WT mouse 14 days after injection of GFP-AAV into the deep cerebellar nucleus. GFP expression (left, green), calbindin expression (middle, red; to stain all Purkinje cells), and merged (right) images are shown. Of 112 calbindin-positive cells, 93 were found to be GFP-positive, indicating ~83% AAV transduction efficiency.
Scale bar = 20 μM
(F) Data corresponding to **Figure 2K**, showing no significant change in firing frequency between groups upon treatment with AAV. WT + GFP-AAV cells: n=22, fxSCA7 92Q + GFP-AAV cells: n=22, fxSCA7 92Q + BK-AAV cells: n=21. One-way ANOVA with Holm-Sidak post-test, *P* = n.s. Error bars = s.e.m.
(G) Representative image of primary cerebellar granule cell neurons loaded with Fluo-4, prior to potassium chloride treatment. Scale bar = 10 μM
(H) Representative image of primary cerebellar granule cell neurons loaded with Fluo-4, after potassium chloride treatment. Scale bar = 10 μM

Figure 4. Expression analysis of Sirt1 over-expression transgenic mice, and rotarod analysis of progeny from the cross of Sirt1 uOE mice with SCA7-266Q mice.
[Related to Figure 4]
(A) To derive transgenic mice that ubiquitously over-express Sirt1, we crossed a line of floxed STOP – Sirt1 transgenic mice (fxSTOP-Sirt1) with CMV-Cre driver mice to yield bigenic mice with excision of the floxed STOP cassette in all tissues, including the CNS and the germ line. Immunoblotting analysis of the resultant bigenic mice (Sirt1 uOE) and parental fxSTOP-Sirt1 mice for Sirt1 was performed as shown, and the expression of Sirt1, relative to β-actin, quantified. We documented a ~3-fold increase in Sirt1 expression in cerebellum and cortex, and a ~2.5-fold increase in Sirt1 expression in the retina. fxSTOP-Sirt1: n = 3, Sirt1-uOE (CMV-Cre x Sirt1): n = 4; two-tailed *t*-test, ***P* <0.01, *****P* <0.0001.
(B) We performed accelerating rotarod analysis on cohorts of mice (n = 6 – 12 / group), of the indicated genotypes at 20 weeks of age, 28 weeks of age, and 36 weeks of age, and compared the

change in latency to fall for the different cohorts for the 20 week to 28 week interval (left) and for the 28 week to 36 week interval (right). While both fxSCA7 92Q mice and Sirt1 uOE – fxSCA7 92Q mice performed significantly worse than control WT and Sirt1 uOE mice for the 20 – 28 week interval, only the fxSCA7 92Q mice performed significantly worse than control WT and Sirt1 uOE mice for the 28 – 36 week interval. One-way ANOVA with post-test Tukey test, $^{**}P < 0.01$. Error bars = s.e.m.

Figure 5. Characterization of progeny from crosses of Sirt1 uOE with SCA7 mice, and time course of calcium homeostasis gene expression changes for Sirt1 uOE transgenic mice. [Related to Figure 4]

(A) Comparison of the age at death for cohorts of littermate SCA7 266Q knock-in mice and Sirt1 uOE-SCA7 266Q bigenic mice. SCA7: n = 21, Sirt1-SCA7: n = 32; two-tailed *t*-test, $^{**}P < 0.01$.

(B) We performed immunoblotting analysis for Sirt1 on cerebellar tissue obtained from cohorts of mice of the indicated ages and genotypes (n = 6 mice / genotype-time point), and then quantified the expression of Sirt1, relative to β-actin. Sirt1 transgenic expression remained ~2.5 – 5-fold the level of endogenous Sirt1 in Sirt1 uOE – fxSCA7 92Q bigenic mice, as they aged. Statistical comparison of Sirt1 expression in Sirt1 uOE – fxSCA7 92Q mice for the different ages indicated that Sirt1 expression levels were similar. ANOVA, $P = 0.717$.

(C) We performed qRT-PCR analysis on RNAs isolated from cerebellar tissue from Sirt1 uOE mice and WT control mice (n = 6 / genotype) at the indicated ages; three technical replicates; two-tailed *t*-test, $^{*}P < 0.05$, $^{**}P < 0.01$. Error bars = s.e.m.

Figure 6. Purkinje cell physiology studies reveal similar membrane excitability in Sirt1uOE and WT mice. [Related to Figure 5]

(A) Purkinje cell firing frequency was measured using extracellular recordings in cerebellar slices from ~30 week-old fxSCA7 92Q mice (n = 11), Sirt1 uOE – fxSCA7 92Q (n = 9), and WT control mice (n = 8). WT cells: n=43, fxSCA7 92Q cells: n=64, Sirt1 uOE – fxSCA7 92Q cells: n=61; *P* = n.s. (not significant), one-way ANOVA with Holm-Sidak post-test.

(B) Representative traces of Purkinje cell firing for ~30 week-old Sirt1 uOE and WT mice.

(C) Purkinje cell firing frequency was measured using extracellular recordings in cerebellar slices from ~30 week-old Sirt1 uOE mice (n = 8) and WT mice (n = 8). WT cells: n=43, Sirt1 uOE cells: n=47; *P* = n.s., two-tailed *t*-test.
(D) The coefficient of variation (CV) of the interspike interval (ISI) of Purkinje cell firing in ~ 30 week-old Sirt1 uOE mice (n = 8) and WT mice (n = 8) is similar. WT cells: n=43, Sirt1 uOE cells: n=47; *P* = n.s., two-tailed *t*-test.
(E) Distribution of ISI CV of Purkinje cell firing from recorded Purkinje cells of Sirt1 uOE and WT mice.
(F) Representative overlaid traces of individual spikes from Purkinje cells of ~ 30 week-old Sirt1 uOE and WT control mice.
(G) In spikes generated in the whole-cell patch-clamp configuration from Purkinje cells in cerebellar slices from ~30 week-old Sirt1 uOE mice (n = 8) and WT mice (n = 8), the decay of the after hyper-polarization (AHP) was indistinguishable. The AHP amplitude was measured at defined points in the Inter Spike Interval (ISI): maximal AHP, mean ISI*0.5, mean ISI*0.65, and mean ISI*0.85. WT cells: n=32, Sirt1 uOE cells: n=40; *P* = n.s., two-way repeated-measures ANOVA with Holm-Sidak post-test. Error bars = s.e.m.

Figure 7. Effect of NMNAT1 nicotinamide pathway enzyme expression and Sirt1 over-expression on NAD^+ levels. [Related to Figure 6]
(A) We performed qRT-PCR analysis on RNA's isolated from cerebellar tissue mice from 36 week-old fxSCA7 92Q and WT control mice (n = 6 / genotype) for each of the NMNAT genes (1, 2, and 3, as indicated); three technical replicates; two-tailed *t*-test, ****P <0.0001.
(B) Quantification of NAD^+ in cerebellar granule cell neurons subjected to mock transfection (Control) or siRNA knock-down of NMNAT1 (NMNAT1 siRNA); n = 4 technical replicates; two-tailed *t*-test, **P <0.01.
(C) We isolated the cerebellum from 36 week-old Sirt1 uOE mice (n=5), fxSCA7 92Q mice (n=5), Sirt1 uOE – fxSCA7 92Q bigenic mice (n=5), and WT controls (n=7), and then performed mass spectrometry measurement of NAD^+ levels. ANOVA with post-hoc Tukey test, **P <0.01.
(D) We transfected neuronal progenitor cells (NPCs) from SCA7 patients or from related, unaffected controls (n = 2 individuals / genotype) with expression constructs for enzymatically

dead Sirt1-HY or Sirt1, and then performed qRT-PCR analysis for Sirt1 on RNA isolates to measure transfection efficiency. Three technical replicates.

(E) We transfected NPCs from SCA7 patients or from related, unaffected controls (n = 2 individuals / genotype) with a PGC-1α shRNA construct, and then performed qRT-PCR analysis for PGC-1α on RNA isolates to knock-down efficiency. Three technical replicates.

Error bars = s.e.m.

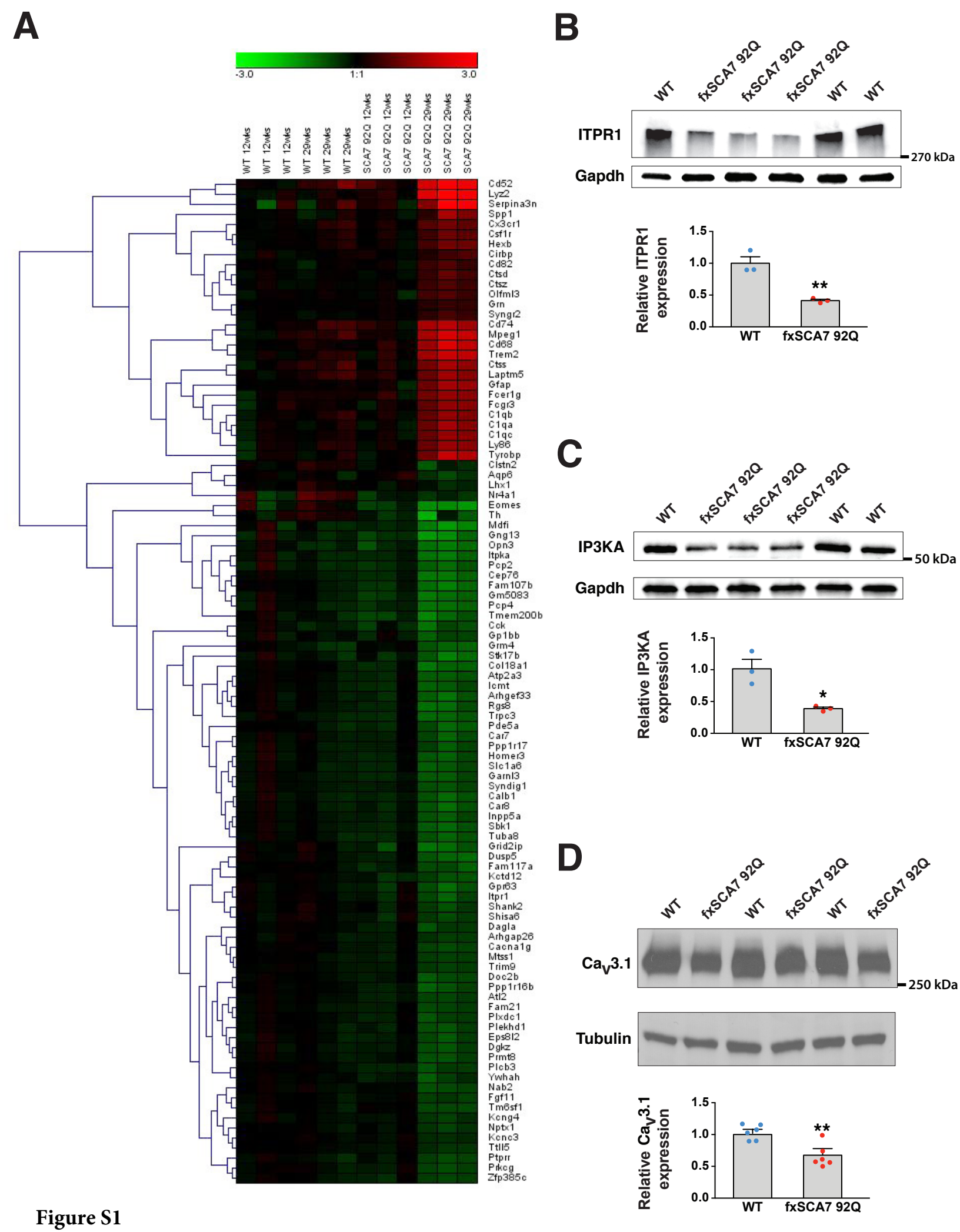
A
-3.0
1:1
3.0
WT 12wks
WT 12wks
WT 12wks
WT 29wks
WT 29wks
WT 29wks
SCA7 92Q 12wks
SCA7 92Q 12wks
SCA7 92Q 12wks
SCA7 92Q 29wks
SCA7 92Q 29wks
SCA7 92Q 29wks
Cd52
Lyz2
Serpina3n
Spp1
Cx3cr1
Csf1r
Hexb
Cirbp
Cd82
Ctsd
Ctsz
Olfml3
Grn
Syngr2
Cd74
Mpeg1
Cd68
Trem2
Ctss
Laptm5
Gfap
Fcer1g
Fcgr3
C1qb
C1qa
C1qc
Ly86
Tyrobp
Clstn2
Aqp6
Lhx1
Nr4a1
Eomes
Th
Mdfi
Gng13
Opn3
Itpka
Pcp2
Cep76
Fam107b
Gm5083
Pcp4
Tmem200b
Cck
Gp1bb
Grm4
Stk17b
Col18a1
Atp2a3
Icmt
Arhgef33
Rgs8
Trpc3
Pde5a
Car7
Ppp1r17
Homer3
Slc1a6
Garnl3
Syndig1
Calb1
Car8
Inpp5a
Sbk1
Tuba8
Grid2ip
Dusp5
Fam117a
Kctd12
Gpr63
Itpr1
Shank2
Shisa6
Dagla
Arhgap26
Cacna1g
Mtss1
Trim9
Doc2b
Ppp1r16b
Atl2
Fam21
Plxdc1
Plekhd1
Eps8l2
Dgkz
Prmt8
Plcb3
Ywhah
Nab2
Fgf11
Tm6sf1
Kcng4
Nptx1
Kcnc3
Ttll5
Ptprr
Prkcg
Zfp385c
B
WT
fxSCA7 92Q
fxSCA7 92Q
fxSCA7 92Q
WT
WT
ITPR1
270 kDa
Gapdh
Relative ITPR1 expression
1.5
1.0
0.5
0.0
**
WT
fxSCA7 92Q
C
WT
fxSCA7 92Q
fxSCA7 92Q
fxSCA7 92Q
WT
WT
IP3KA
50 kDa
Gapdh
Relative IP3KA expression
1.5
1.0
0.5
0.0
*
WT
fxSCA7 92Q
D
WT
fxSCA7 92Q
WT
fxSCA7 92Q
WT
fxSCA7 92Q
CaV3.1
250 kDa
Tubulin
Relative CaV3.1 expression
1.5
1.0
0.5
0.0
**
WT
fxSCA7 92Q

Figure S1

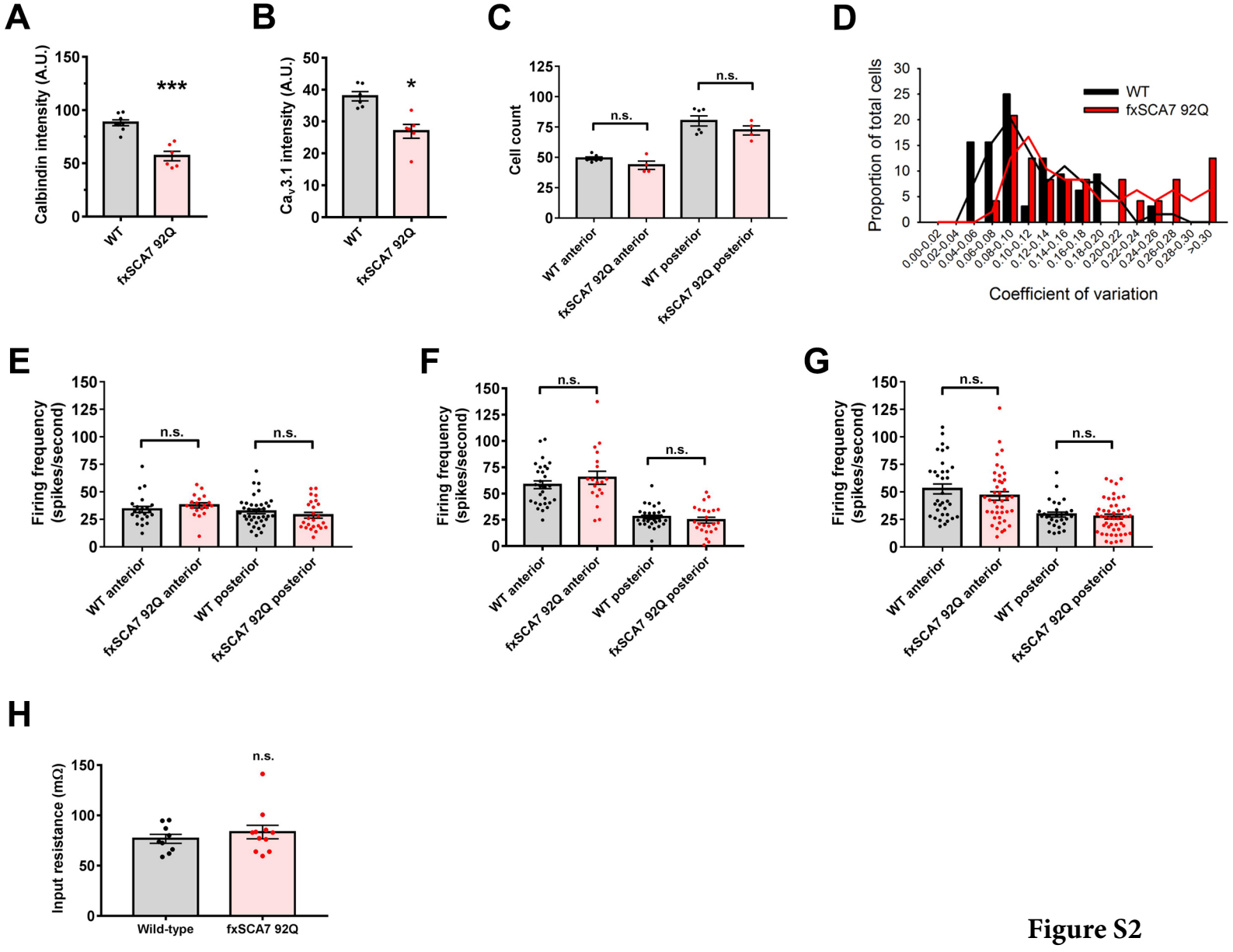
A
Calbindin intensity (A.U.)
150
100
50
0
***
WT
fxSCA7 92Q
B
Ca$_v$3.1 intensity (A.U.)
50
40
30
20
10
0
*
WT
fxSCA7 92Q
C
Cell count
125
100
75
50
25
0
n.s.
n.s.
WT anterior
fxSCA7 92Q anterior
WT posterior
fxSCA7 92Q posterior
D
Proportion of total cells
30
25
20
15
10
5
0
WT
fxSCA7 92Q
0.00-0.02
0.02-0.04
0.04-0.06
0.06-0.08
0.08-0.10
0.10-0.12
0.12-0.14
0.14-0.16
0.16-0.18
0.18-0.20
0.20-0.22
0.22-0.24
0.24-0.26
0.26-0.28
0.28-0.30
>0.30
Coefficient of variation
E
Firing frequency (spikes/second)
150
125
100
75
50
25
0
n.s.
n.s.
WT anterior
fxSCA7 92Q anterior
WT posterior
fxSCA7 92Q posterior
F
Firing frequency (spikes/second)
150
125
100
75
50
25
0
n.s.
n.s.
WT anterior
fxSCA7 92Q anterior
WT posterior
fxSCA7 92Q posterior
G
Firing frequency (spikes/second)
150
125
100
75
50
25
0
n.s.
n.s.
WT anterior
fxSCA7 92Q anterior
WT posterior
fxSCA7 92Q posterior
H
Input resistance (mΩ)
150
100
50
0
n.s.
Wild-type
fxSCA7 92Q

Figure S2

Figure S3

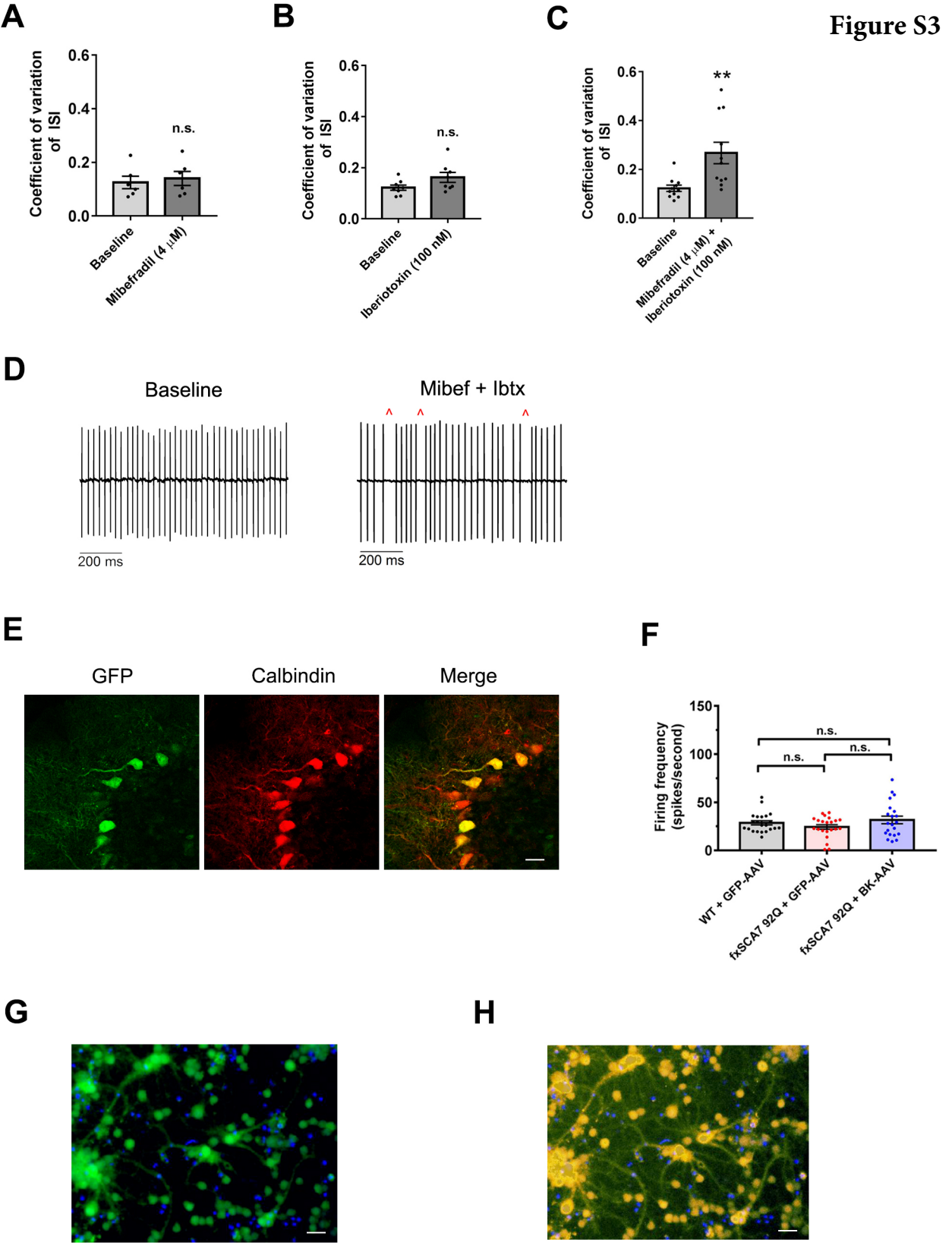
A
Coefficient of variation of ISI
0.6
0.4
0.2
0.0
n.s.
Baseline
Mibefradil (4 μM)
B
Coefficient of variation of ISI
0.6
0.4
0.2
0.0
n.s.
Baseline
Iberiotoxin (100 nM)
C
Coefficient of variation of ISI
0.6
0.4
0.2
0.0
**
Baseline
Mibefradil (4 μM) + Iberiotoxin (100 nM)
D
Baseline
Mibef + Ibtx
200 ms
200 ms
E
GFP
Calbindin
Merge
F
Firing frequency (spikes/second)
150
100
50
0
n.s.
n.s.
n.s.
WT + GFP-AAV
fxSCA7 92Q + GFP-AAV
fxSCA7 92Q + BK-AAV
G
H

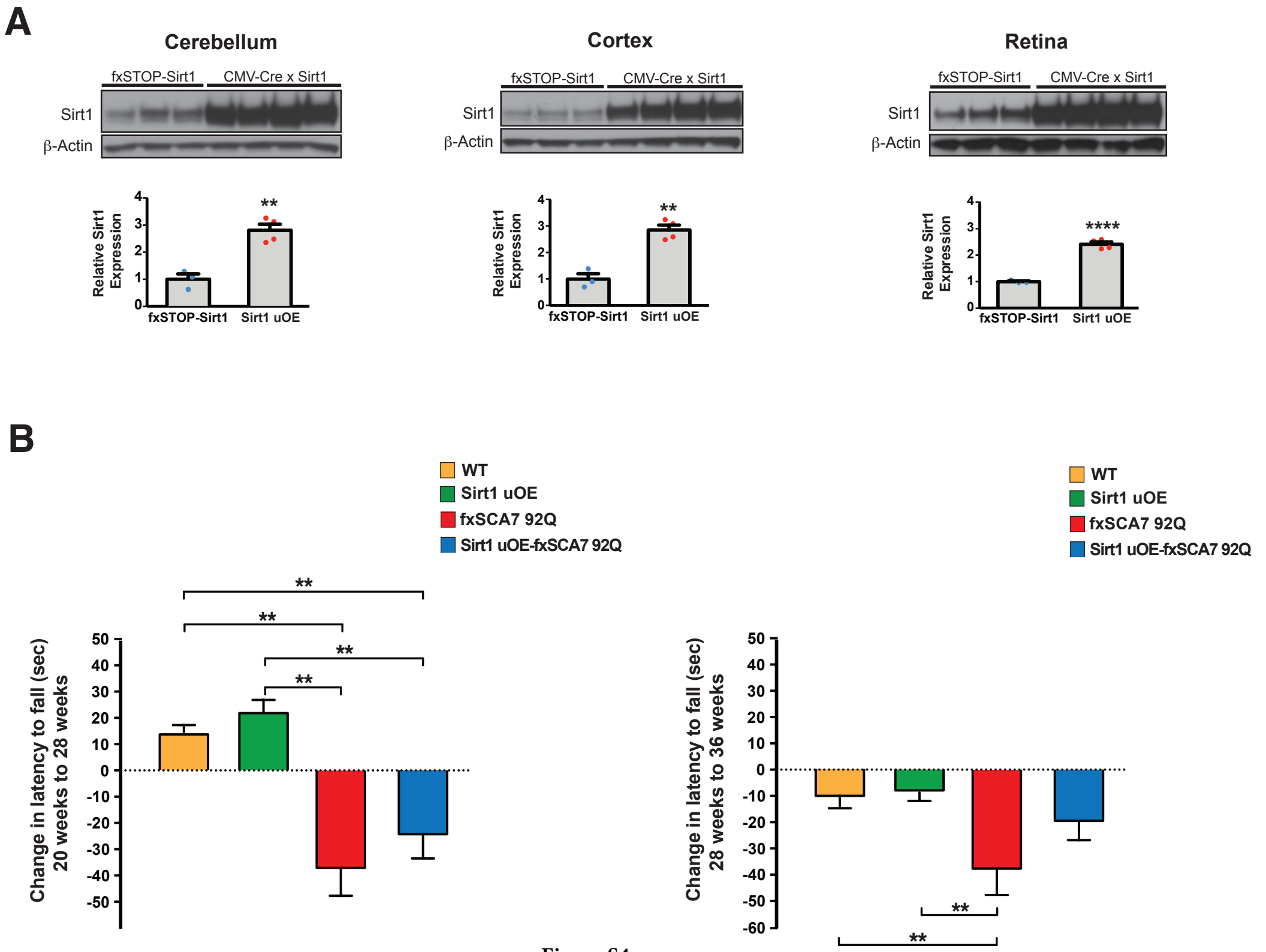
A
Cerebellum
Cortex
Retina
fxSTOP-Sirt1
CMV-Cre x Sirt1
Sirt1
β-Actin
Relative Sirt1 Expression
fxSTOP-Sirt1
Sirt1 uOE
**
****
B
WT
Sirt1 uOE
fxSCA7 92Q
Sirt1 uOE-fxSCA7 92Q
Change in latency to fall (sec) 20 weeks to 28 weeks
Change in latency to fall (sec) 28 weeks to 36 weeks

Figure S4

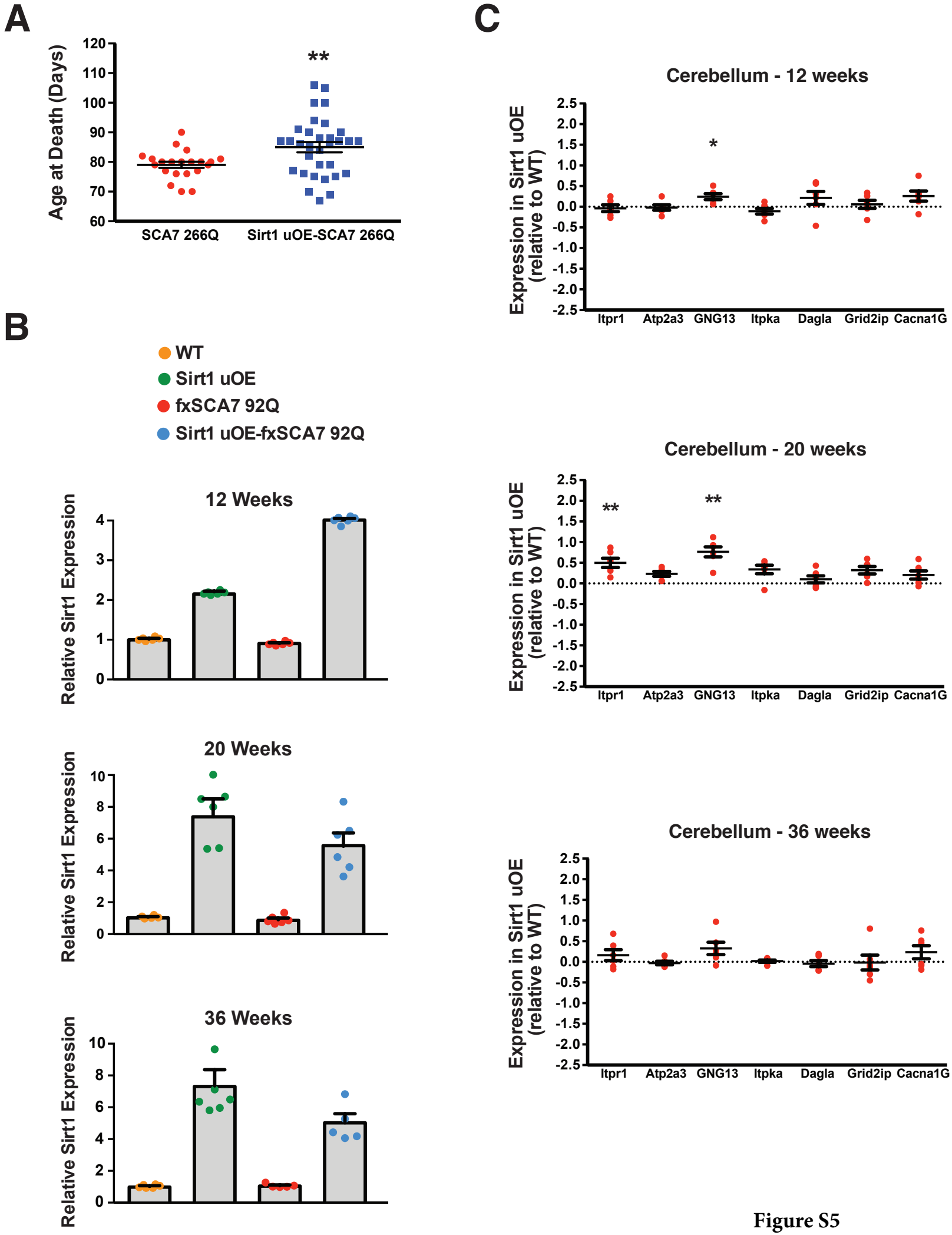
A
Age at Death (Days)
120
110
100
90
80
70
60
**
SCA7 266Q
Sirt1 uOE-SCA7 266Q
B
WT
Sirt1 uOE
fxSCA7 92Q
Sirt1 uOE-fxSCA7 92Q
12 Weeks
Relative Sirt1 Expression
20 Weeks
Relative Sirt1 Expression
36 Weeks
Relative Sirt1 Expression
C
Cerebellum - 12 weeks
Expression in Sirt1 uOE (relative to WT)
*
Cerebellum - 20 weeks
Expression in Sirt1 uOE (relative to WT)
**
**
Cerebellum - 36 weeks
Expression in Sirt1 uOE (relative to WT)
Itpr1
Atp2a3
GNG13
Itpka
Dagla
Grid2ip
Cacna1G

Figure S5

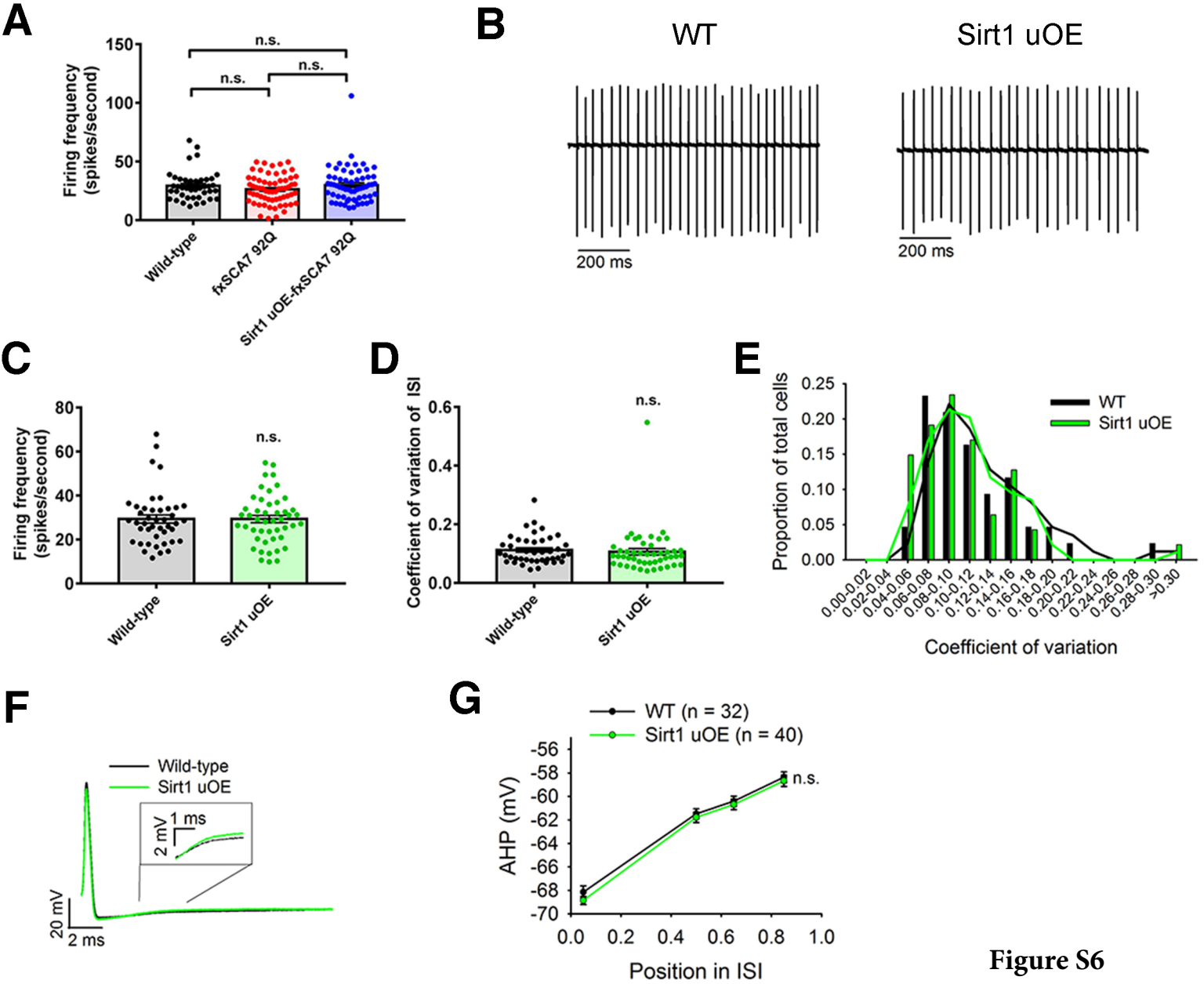
A
Firing frequency (spikes/second)
150
100
50
0
n.s.
n.s.
n.s.
Wild-type
fxSCA7 92Q
Sirt1 uOE-fxSCA7 92Q
B
WT
Sirt1 uOE
200 ms
200 ms
C
Firing frequency (spikes/second)
80
60
40
20
0
n.s.
Wild-type
Sirt1 uOE
D
Coefficient of variation of ISI
0.6
0.4
0.2
0.0
n.s.
Wild-type
Sirt1 uOE
E
Proportion of total cells
0.25
0.20
0.15
0.10
0.05
0.00
WT
Sirt1 uOE
0.00-0.02
0.02-0.04
0.04-0.06
0.06-0.08
0.08-0.10
0.10-0.12
0.12-0.14
0.14-0.16
0.16-0.18
0.18-0.20
0.20-0.22
0.22-0.24
0.24-0.26
0.26-0.28
0.28-0.30
>0.30
Coefficient of variation
F
Wild-type
Sirt1 uOE
2 mV
1 ms
20 mV
2 ms
G
WT (n = 32)
Sirt1 uOE (n = 40)
AHP (mV)
-56
-58
-60
-62
-64
-66
-68
-70
n.s.
0.0
0.2
0.4
0.6
0.8
1.0
Position in ISI

Figure S6

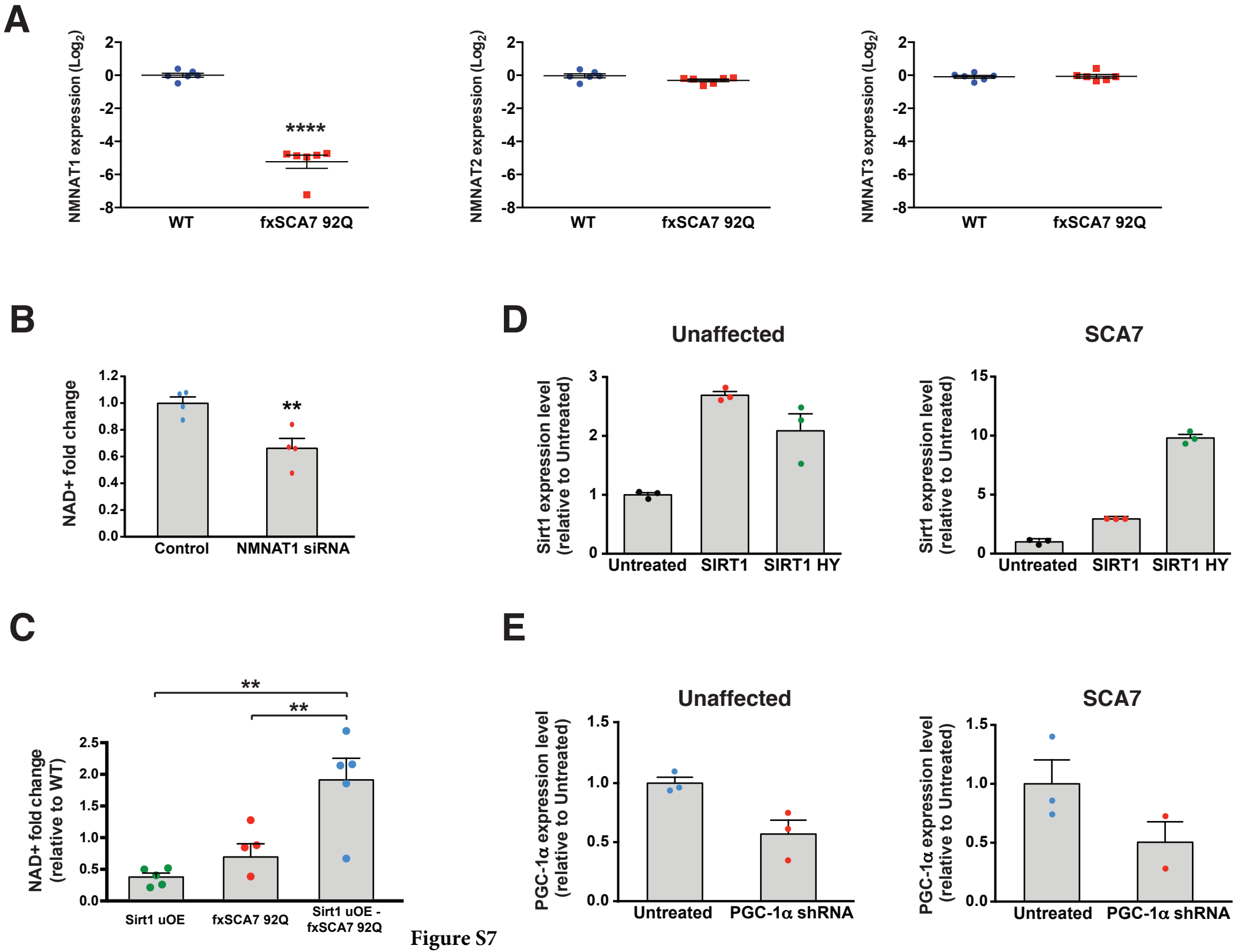
A
NMNAT1 expression (Log2)
2
0
-2
-4
-6
-8
****
WT
fxSCA7 92Q
NMNAT2 expression (Log2)
WT
fxSCA7 92Q
NMNAT3 expression (Log2)
WT
fxSCA7 92Q
B
NAD+ fold change
1.2
1.0
0.8
0.6
0.4
0.2
0.0
**
Control
NMNAT1 siRNA
C
NAD+ fold change (relative to WT)
2.5
2.0
1.5
1.0
0.5
0.0
**
**
Sirt1 uOE
fxSCA7 92Q
Sirt1 uOE - fxSCA7 92Q
D
Unaffected
Sirt1 expression level (relative to Untreated)
3
2
1
0
Untreated
SIRT1
SIRT1 HY
SCA7
Sirt1 expression level (relative to Untreated)
15
10
5
0
Untreated
SIRT1
SIRT1 HY
E
Unaffected
PGC-1α expression level (relative to Untreated)
1.5
1.0
0.5
0.0
Untreated
PGC-1α shRNA
SCA7
PGC-1α expression level (relative to Untreated)
1.5
1.0
0.5
0.0
Untreated
PGC-1α shRNA

Figure S7